PERGAMON

Journal of Structural Geology 25 (2003) 1011–1020

JOURNAL OF STRUCTURAL GEOLOGY

www.elsevier.com/locate/jsg

Critical displacement for normal fault nucleation from en-échelon vein arrays in limestones: a case study from the southern Apennines (Italy)

Stefano Mazzoli[a,*], Daniela Di Bucci[b]

[a]*Facoltà di Scienze Ambientali, Università di Urbino, Campus Scientifico Sogesta, 61029 Urbino (PU), Italy*
[b]*National Seismic Survey, Via Curtatone n. 3, 00185 Rome, Italy*

Received 15 March 2002; revised 16 September 2002; accepted 17 September 2002

Abstract

The process of fault initiation by the coalescence of en-échelon arrays of tensile cracks has been discussed by several workers and is now well established. However, not many studies have tried to quantitatively describe this process in terms of displacement and shear strain that control the early stages of fault nucleation. In this study, a large number of conjugate en-échelon vein arrays showing extensional offsets have been analysed. These structures are exposed in well bedded micritic limestones deformed at very low-grade conditions in the Apennine mountain belt of southern Italy. Three different types of structures can be distinguished: (i) 'brittle–ductile' shear zones, characterised by arrays of en-échelon, calcite-filled tension gashes; (ii) shear zones showing incipient development of discontinuous shear-parallel fractures cutting through the vein array; and (iii) faulted shear zones, in which a continuous, discrete normal fault breaks through—and clearly developed from—an original en-échelon vein array. Critical values of displacement and shear strain have been determined for the onset of normal fault nucleation from 'brittle–ductile' shear zones, therefore suggesting that these parameters exert a major control on fault initiation. A diagram of shear zone population vs. displacement also shows that this parameter obeys a power law of the type generally followed by normal faults in the frictional regime. Our results suggest that, during the early stages of fault nucleation, displacement and shear strain control the switch from dominant ductile (viscous) deformation mechanisms—accompanied by brittle fracturing responsible for vein formation—to the frictional regime.

Keywords: 'Brittle–ductile' shear zones; Fault initiation; Shear strain; Scaling properties; Very low-grade rocks

1. Introduction

The processes of fault nucleation have been intensely investigated in natural fault zones. In recent years, a relevant contribution to the comprehension of strike-slip fault nucleation came from the work of Peacock and Sanderson (1995), Willemse et al. (1997) and Kelly et al. (1998). In all cases, the field examples were characterised by the occurrence of en-échelon vein arrays in conjugate strike-slip fault zones. The observed evolution along these zones from vein arrays to faults allowed the authors to implement a model of linkage in which pull-apart mechanisms play a primary role.

In a more general sense, fault initiation by the coalescence of en-échelon arrays of Mode I (tensile) cracks has been suggested by several authors (e.g. Knipe and White, 1979; Pollard et al., 1982; Etchecopar et al., 1986; Cox and Scholz, 1988a,b) and can also characterise structures other than strike-slip faults (Scholz, 1990 and references therein). However, in spite of the great number of works concerning en-échelon vein arrays, none of them essentially deals with the related shear displacement, and only few scattered data are available. These data are mainly related to limestones (occasionally to shales), and show displacements ranging from about 1 cm for 'brittle–ductile' shear zones (Smith, 1997; Willemse et al., 1997) to tens of centimetres for incipient faults (McGrath and Davison, 1995; Kelly et al., 1998).

In this work, we specifically analyse the process of normal fault initiation from so-called 'brittle–ductile' shear zones (Ramsay and Huber, 1987), characterised by arrays of en-échelon tension gashes. The analysis was carried out quantitatively in terms of the displacements that are necessary to produce (i) the formation of shear-parallel fractures across the vein array, and eventually (ii) linkage of such shear fractures to form a discrete fault zone. The studied structures are hosted in well-bedded, fine-grained

* Corresponding author. Tel./fax: +39-0722-304-295.
E-mail address: s.mazzoli@geo.uniurb.it (S. Mazzoli).

0191-8141/03/$ - see front matter © 2002 Elsevier Science Ltd. All rights reserved.
PII: S0191-8141(02)00156-6

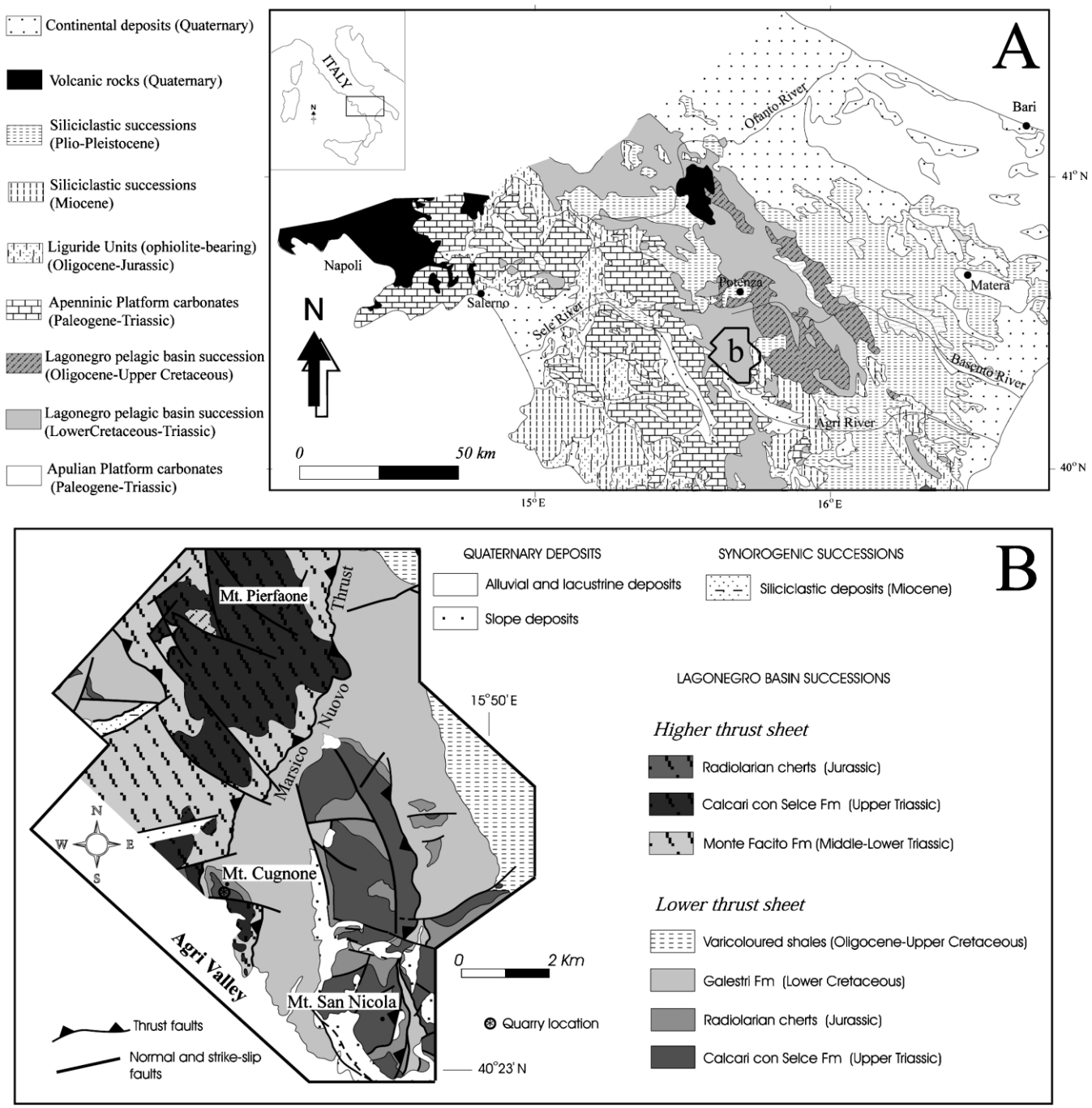

Fig. 1. Location (A) and schematic geological setting (B) of the study area (after Mazzoli et al., 2001 modified).

limestones exposed in a quarry in the southern Apennines of Lucania, Italy (Fig. 1). Traits make this outcrop appropriate for this kind of analysis: (i) numerous conjugate sets of vein arrays are well exposed (Fig. 2A); (ii) some of them show incipient shear fracture development across the tensile cracks; (iii) some of them are definitely faulted (Fig. 2B); (iv) in all instances the displacement can be measured; and (v) the displacement associated with shear zones and faults is quite low (not exceeding 1 m, and mostly below 20 cm). Summing up, different steps of the early stages of nucleation of a normal fault are exposed, hence allowing a comprehensive analysis of displacement accumulation during incipient faulting.

2. Geological setting

The work was carried out in Upper Triassic micritic limestones ('Calcari con selce' formation) from the Mesozoic Lagonegro Basin succession of the southern Apennines fold and thrust belt of peninsular Italy (e.g. Cello and Mazzoli, 1999 and references therein). The limestones

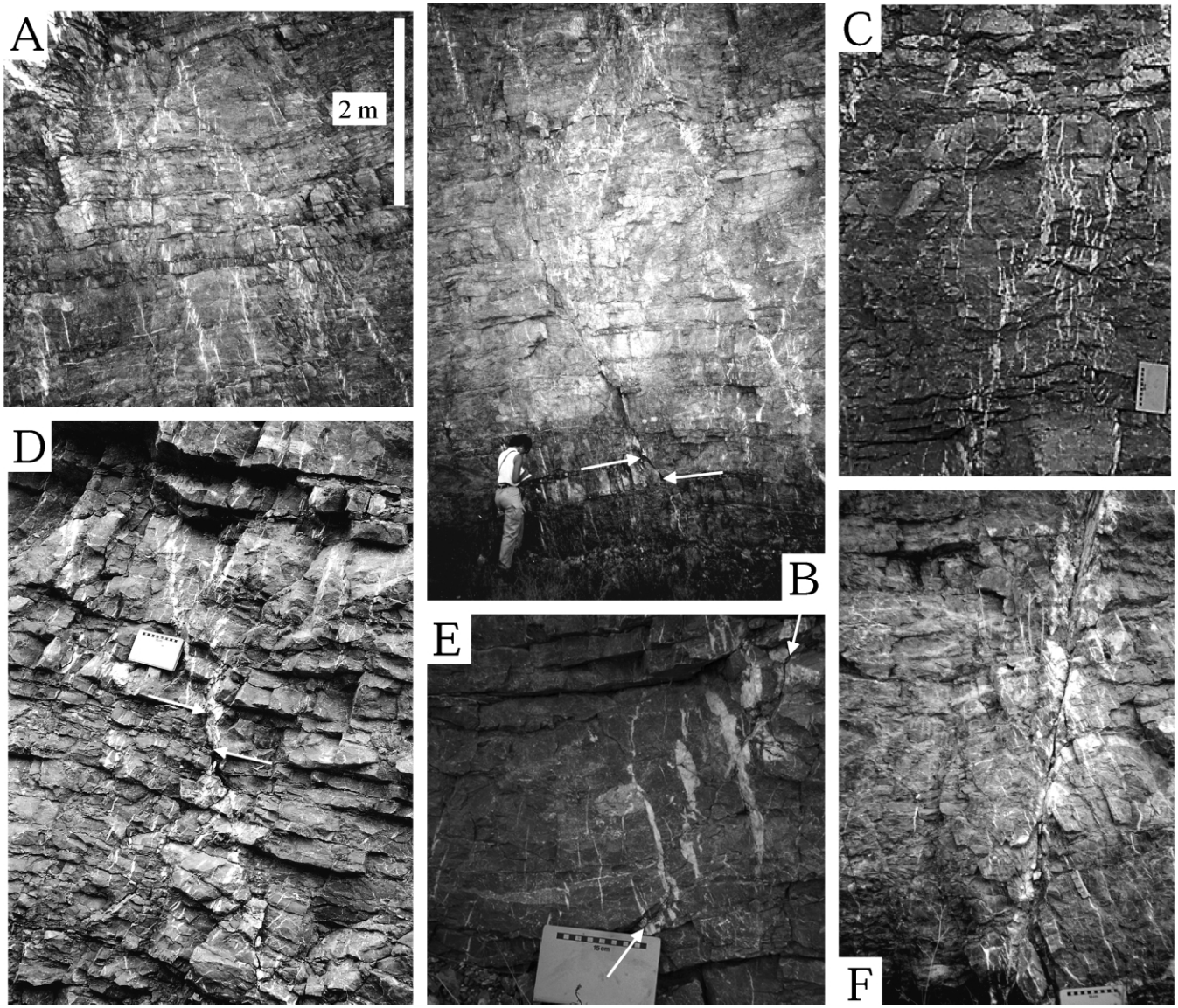

Fig. 2. Examples of different types of analysed structures. (A) View of conjugate 'brittle–ductile' shear zones in the eastern quarry wall. (B) Conjugate 'brittle–ductile' shear zones and faulted shear zone (arrows show displacement). (C) Unbroken, conjugate 'brittle–ductile' shear zones. (D) Shear zone showing incipient development of discontinuous shear-parallel fractures cutting across en-échelon vein array (arrows show displacement along shear fracture). (E) Detail of discontinuous shear-parallel fractures (arrowed) cutting across en-échelon vein array. (F) Faulted shear zone, characterised by a continuous, discrete fault zone breaking through an original en-échelon vein array.

are exposed in a quarry at Monte Cugnone, in the high Agri Valley of Lucania (Fig. 1). Structural analysis indicates that this formation, a few hundreds of metres thick, represented the mechanically dominant member during contraction and buckling of the sedimentary multilayer, which led to the formation of NW–SE to N–S-trending, flexural-slip-dominated folds in this area (Mazzoli et al., 2001).

The Monte Cugnone regional structure consists of a faulted anticline of about 1 km wavelength, exposed in the footwall to a major thrust within the Lagonegro units (Marsico Nuovo Thrust; Fig. 1B). Overprinting relationships indicate that the extensional structures analysed in this study post-dated both (i) layer parallel shortening-related features, and (ii) fold-related flexural-slip deformation. Therefore, they can be best related to a post-contraction extensional deformation that, at least within the studied outcrop, appears to accommodate a relatively low amount of strain. Environmental (P–T) conditions in existence during the development of the shear zones were mostly controlled by the tectonic burial resulting from the previous contractional episodes (Mazzoli et al., 2001). Maximum homogenisation temperatures from primary fluid inclusions in vein calcite are mostly in the range of 130–140 °C (Invernizzi, 2002). Environmental conditions remained constant during the different stages of shear zone evolution and normal fault development (Invernizzi, 2002), implying substantial exhumation after the formation of the investigated structures.

The area of our detailed study is located in the crestal region of the gently northwest-plunging Monte Cugnone anticline, in a sector of the major fold characterised by sub-horizontal to gently dipping bedding. The quarry is developed with three well-exposed quarry walls; one roughly WSW–ENE oriented, the other two trending NNW–SSE. The latter two quarry sides are approximately perpendicular to the strike of the shear zones, providing the best exposures for their study (Fig. 2); in detail, outcrop surfaces are differently oriented and quite irregular, permitting correct measurement of veins and arrays as required for geometrical analysis (Smith, 1995). The host rock consists of a strongly anisotropic but rather homogeneous multilayer, characterised by regular limestone beds (mostly 10–40 cm thick) containing chert lenses and nodules. The portion of 'Calcari con selce' Fm exposed in the quarry is completely lacking in the marly/clayey intercalations that are typical of other parts of this formation (Mazzoli et al., 2001). This rules out the possibility that the localisation of 'brittle–ductile' shear zones and discrete faults is controlled by competence contrasts between layers of differing composition.

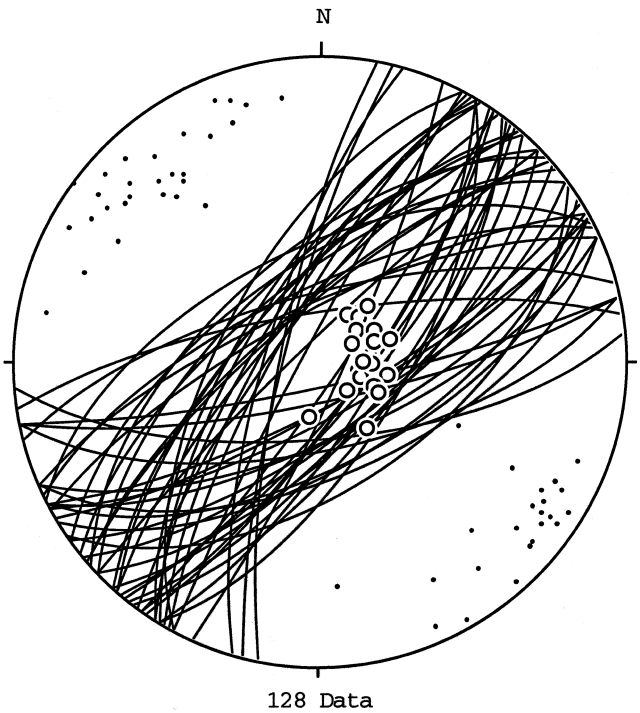

Fig. 3. Orientation data (lower hemisphere, equal area projection) for: (i) shear zones (great circles), (ii) average attitude of tension gashes from en-échelon vein arrays (poles to vein planes; dots), and (iii) bedding (poles to planes; circles). For the few non-planar (sigmoidal) veins observed in the field, plotted data refer to the vein tip area (i.e. to the non-rotated part of the vein).

3. Shear zone characteristics

3.1. Data acquisition

Fifty-four shear zones of extensional type, exposed over lengths of several metres to a few tens of metres, have been analysed. Most of the shear zones are arranged in conjugate sets, generally striking NE–SW and dipping on average 73° toward both NW and SE. Conjugate shear zones are in general equally well developed, suggesting conditions of bulk coaxial strain for their development (Ramsay and Graham, 1970). Conjugate shear zone intersections are generally sub-horizontal to gently plunging and approximately lie in the bedding planes, which in turn display very low dips (Fig. 3). This provided the opportunity to carry out accurate measurements of shear zone displacement using bedding as a marker.

Stylolites—recognised on the basis of their sutured shape and the presence of residual material—are commonly found parallel to bedding and are best interpreted as diagenetic in origin (Bathurst, 1971). En-échelon extension veins are generally observed to cut across bedding-parallel stylolites, or, occasionally, to be truncated by them. The latter relationship can be the effect of pre-existing discontinuities (i.e. the stylolites) inhibiting the propagation of later extension fractures (e.g. Price and Cosgrove, 1990). However, in some instances bedding-parallel stylolites can be clearly observed cutting across (otherwise continuous) extension veins. This feature indicates that bedding-parallel stylolites, maintaining a suitable orientation relative to vertical loading, were also reactivated during extensional deformation. The related pressure-solution process possibly provided the source of material for calcite precipitation in nearby tension gashes.

Most en-échelon vein arrays are intimately associated with the shear zones (Fig. 2) and possibly represent original zones of weakness that localised later shear zone development (e.g. Roering, 1968; Olson and Pollard, 1991 and references therein). The veins, filled with calcite, consist of a thick central portion that tapers off into narrow tails. They are usually planar and only in few cases show a sigmoidal shape (most probably due to rotation of their central part as a result of shearing; Ramsay and Graham, 1970). In profile, veins are generally tens of centimetres in length and have maximum aperture width of a few centimetres. Single veins measured from en-échelon arrays strike NE–SW and dip on average 74° toward both NW and SE (Fig. 3). Compared with the shear zone attitude, the vast majority of the measured vein arrays can be geometrically classified, according to Beach (1975), as 'Type 1' (adopted as a strictly descriptive term, and not referring to the mode of formation of the vein arrays). They mostly range from the 'weakly convergent' to the 'strongly convergent' types of Smith (1996).

We distinguished: (i) unbroken 'brittle–ductile' shear zones, characterised by arrays of en-échelon, calcite-filled tension gashes (Fig. 2C); (ii) shear zones showing discontinuous shear-parallel fractures cutting across the vein array (Fig. 2D and E); and (iii) faulted shear zones,

Table 1
Structural data. α = angle between bedding and shear zone; θ = average angle between shear zone and associated veins; γ = shear strain. See text for discussion on shear strain data from faults

Type	Shear zone attitude		Average vein attitude		α	θ	Thickness	Displacement	γ
	Dip direction	Angle of dip	Dip direction	Angle of dip			(cm)	(cm)	
Shear zone	298	86	122	77	82	19	4.9	0.1	0.02
Shear zone	284	81	100	80	64	20	4.8	1.1	0.23
Shear zone	311	71	149	76	60	38	12	1.2	0.09
Shear zone	130	76	304	84	82	21	3.6	1.5	0.42
Shear zone	125	78	291	80	81	27	3.2	1.5	0.48
Shear zone	152	62	330	87	68	32	3.7	1.6	0.44
Shear zone	168	83	355	63	80	34	3.4	2	0.61
Shear zone	145	56	217	76	64	67	8.3	2.2	0.27
Shear zone	281	80	118	82	63	26	5.3	2.2	0.43
Shear zone	316	66	136	81	64	34	4.2	2.2	0.53
Shear zone	299	79	310	74	66	12	2.7	2.2	0.81
Shear zone	324	65	127	80	58	40	9.6	2.4	0.24
Shear zone	156	69	161	79	81	11	1	2.5	2.65
Shear zone	124	78	298	79	89	25	7.2	3	0.42
Shear zone	140	71	311	81	88	31	6.2	3	0.49
Shear zone	152	70	336	84	81	27	5	3	0.61
Shear zone	321	69	131	82	72	31	13	3.2	0.24
Fault	302	69	129	71	64	42	6.7	3.3	0.5
Shear zone	128	71	138	68	86	10	2.6	3.5	1.35
Shear zone	331	77	141	75	55	31	15	3.7	0.24
Shear zone	149	78	133	74	89	16	4.1	4	0.97
Shear zone	121	67	304	77	80	38	4.3	4.1	0.94
Shear zone	156	59	297	76	52	59	13	4.4	0.35
Shear zone	286	76	111	71	64	34	9.5	4.5	0.47
Shear zone	168	66	332	70	70	46	4.3	4.8	1.11
Incipient fault	127	68	304	74	77	39	8.8	5	0.57
Shear zone	121	74	318	87	87	26	5.7	5	0.88
Shear zone	144	71	126	89	68	26	11	5.4	0.49
Shear zone	311	77	299	62	62	18	3.4	5.7	1.67
Shear zone	148	62	164	76	73	21	7.2	5.8	0.8
Shear zone	351	77	172	76	87	28	3.8	6	1.6
Shear zone	312	71	131	71	64	38	9.2	6.7	0.72
Shear zone	334	71	144	53	59	58	7.6	7.6	0.99
Shear zone	300	76	126	75	66	31	11	7.7	0.71
Shear zone	318	62	154	71	41	50	6.1	8.4	1.37
Incipient fault	302	74	121	66	57	40	19	8.9	0.46
Shear zone	345	72	149	76	65	36	7.6	9.4	1.23
Shear zone	336	75	160	72	71	34	21	9.5	0.46
Fault	129	78	302	76	89	28	7	9.5	1.35
Fault	125	84	295	42	86	55	5.3	9.5	1.79
Shear zone	298	64	129	71	46	47	11	9.7	0.89
Fault	151	75	300	73	75	45	9.2	11	1.24
Shear zone	132	71	306	79	80	30	4.5	11	2.48
Incipient fault	168	79	322	75	70	37	8.4	13	1.52
Incipient fault	301	71	142	67	60	47	11	14	1.26
Fault	306	79	137	64	63	40	8.4	16	1.88
Shear zone	319	77	139	61	62	44	17	17	0.98
Fault	114	83	304	81	86	19	5.2	30	5.68
Fault	333	60	158	81	39	39	5	30	6
Incipient fault	319	76	144	65	76	40	9	40	4.47
Fault	152	78	318	64	73	41	9.8	41	4.14
Fault	175	69	310	81	87	54	8.9	43	4.84
Fault	136	69	301	85	66	30	7.5	44	5.84
Fault	316	85	143	63	73	33	6.5	99	15.2

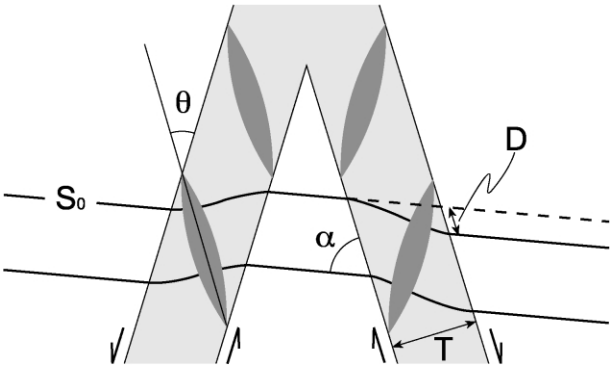

Fig. 4. Schematic diagram of conjugate 'brittle–ductile' shear zones, showing measured parameters T (shear zone thickness) and D (shear zone displacement). S_0 = bedding; α = angle between bedding and shear zone; θ = average angle between shear zone and associated veins.

characterised by a continuous, discrete fault zone breaking through—and clearly developed from—an original en-échelon vein array (Fig. 2F). These discrete fault zones, in turn, are very likely to have formed by linkage of pre-existing shear fractures of the type shown in Fig. 2D and E, so that a progressive evolution appears to occur from (i) to (ii), to (iii) above. For each shear zone, we measured attitude, thickness and displacement (Table 1), as well as bedding attitude. Shear zone thickness (T) has been measured as the perpendicular distance between the two enveloping surfaces containing the tip lines of the tension gashes belonging to a single array (Fig. 4). Shear zone displacement (D) has been measured, using the trace of offset bedding, in the XZ plane of the related finite strain ellipsoid and along the shear direction (assuming that the intersection of conjugate shear zones is parallel to the intermediate (Y) axis of the related finite strain ellipsoid; Ramsay and Huber, 1987). The shear strain (γ) can then be obtained for each shear zone simply as (Fig. 4):

$$\gamma = D/T \quad (1)$$

Eq. (1) permits the determination of γ also for shear zones showing incipient development of shear-parallel fractures (Fig. 2D and E) or that have completely evolved to discrete faults (Fig. 2F). In the latter instances, the measured shear zone thickness (T) is that of the whole shear zone from which the fault zone has developed, whereas the displacement (D) is the cumulative offset of bedding due to both 'brittle–ductile' deformation and subsequent fault-related slip. By this method, the related shear strain (γ) is determined as if all the deformation was of ductile nature and occurring across the whole thickness (T) of the shear zone. For broken (i.e. faulted) shear zones, this method introduces an approximation which will be taken into account in the following analysis.

3.2. Data analysis

Analysis of shear zone displacement (D) indicates that a critical value of ca. 9 cm offset can be identified for significant onset of normal fault nucleation from 'brittle–ductile' shear zones in the studied limestones (Fig. 5A). Below this value, the development of discontinuous shear-parallel fractures or through-going faults occurs only in two instances out of 35. Displacement values in the range of 9–17 cm appear to characterise a 'transition zone' to the development of discrete faults. Within this zone, different types of structures, ranging from unbroken 'brittle–ductile' shear zones to completely faulted ones, occur. For displacement values in excess of 17 cm, almost exclusively broken (i.e. faulted) shear zones occur.

For the determination of possible critical values of shear strain for normal fault nucleation from 'brittle–ductile' shear zones, the approximation introduced in the calculation of γ from broken (i.e. faulted) shear zones must be taken into account. For these structures, the following would be needed: (i) an accurate partitioning of the total displacement into components associated with the original 'brittle–ductile' deformation and the (later) through-going fault; and (ii) an estimate of the thickness of the shear zone at the time of fault formation. The unknown, possibly complex structural evolution that took place as a result of displacement localisation during overall strain accumulation in these structures clearly inhibits the analyses above. However, it should be noted that, for the faulted shear zones investigated in this study, we are dealing with very limited values of displacement (of a few tens of centimetres at most; Table 1). Therefore, as a first approximation, we assume that shear zone characteristics—specifically thickness, upon which the shear strain is dependent—are quite close to those at the time of fault formation. Given this, the method adopted in the calculation of γ is likely to lead to a progressively larger underestimation of the shear strain as deformation localises along a discrete fault zone (with the consequent narrowing of the actual slip zone thickness). Therefore, our method is likely to represent a conservative approach for the determination of the cumulative shear strain in faulted shear zones. The consequences of this approximation in the determination of γ appear to be negligible in a diagram like that of Fig. 5B. In fact, a possible underestimation of the shear strain for the larger faults (i.e. those in the right-hand side of the diagram) would not substantially affect the histogram pattern of Fig. 5B. The latter suggests that significant normal fault nucleation starts to occur for shear strain values around 1.2. Therefore, it seems that shear strains in the range of $0 < \gamma < 1.2$ can be sustained by the shear zones, without significant development of shear parallel fractures cutting across the tensile crack array (which is shown to have occurred in three instances out of 35). Above $\gamma \approx 1.2$, structures of different types (unbroken, incipiently faulted and faulted shear zones) appear to define again a transition zone to the development of discrete faults. For γ values above 2.7, relatively high values of shear strain are mostly taken up by through-going, discrete faults.

The scaling properties of shear zone displacement have

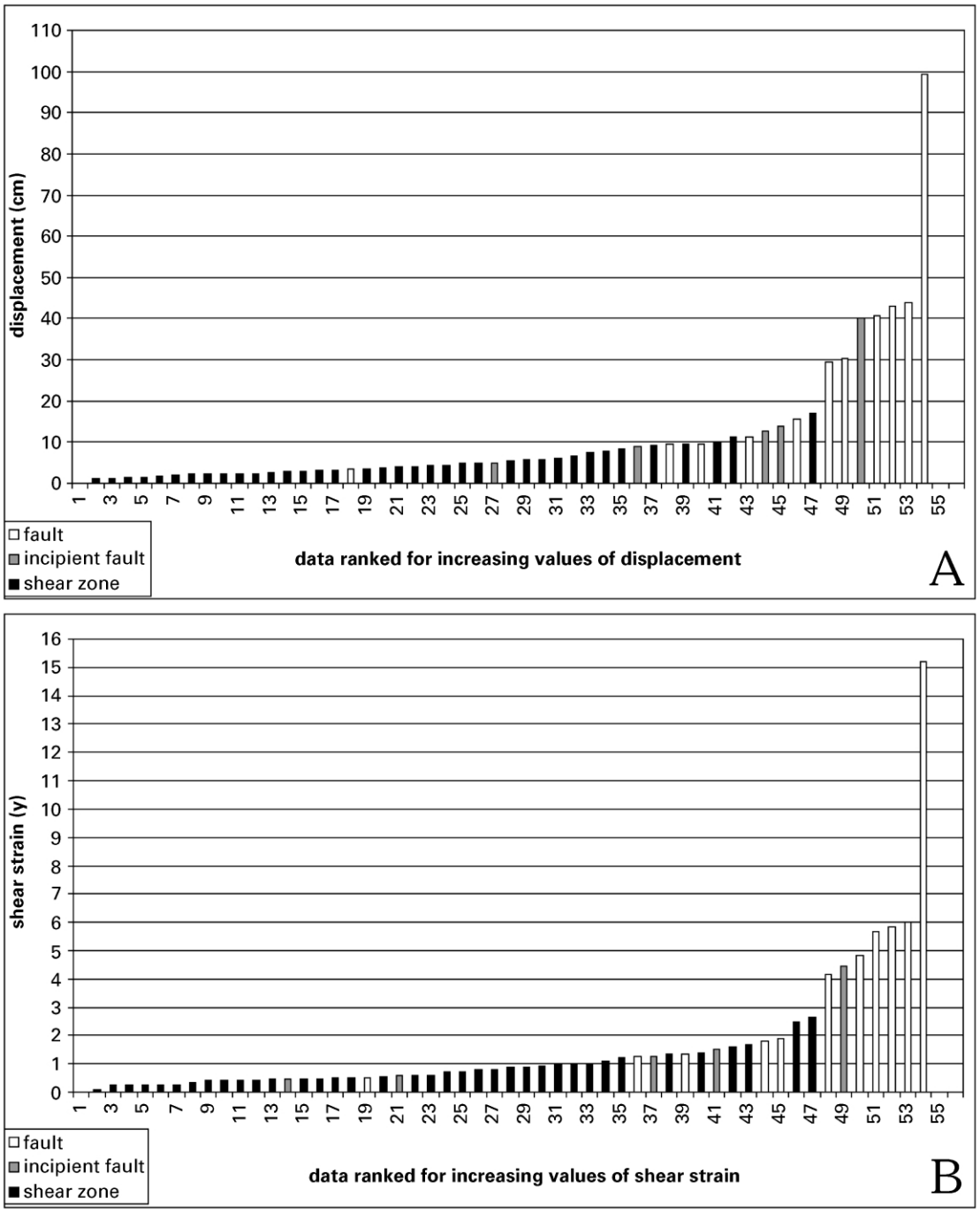

Fig. 5. Histograms of shear zone displacement (A) and shear strain (B).

also been investigated. It is well known that this parameter, as well as others measured from many sampled fault populations, tend to be self-similar over a wide range of scales. Fault populations are generally described by a power-law frequency distribution of the form (e.g. Needham et al., 1996; Yielding et al., 1996 and references therein):

$$N = aS^{-d} \tag{2}$$

where N is the number of features having a size greater than or equal to S (e.g. fault displacement). The variable a is a measure of the size of the sample, and the power-law exponent d is termed the fractal dimension of the population.

The 54 shear zones analysed in this study provide a data set that is similar in size to those included in published accounts on scaling properties of fault throw/displacement (e.g. Knott et al., 1996; Needham et al., 1996). This permits a comparison of the behaviour shown by discrete faults in the literature with that of the studied 'brittle–ductile' shear zones. For these, the graph (on logarithmic axes) of cumulative number

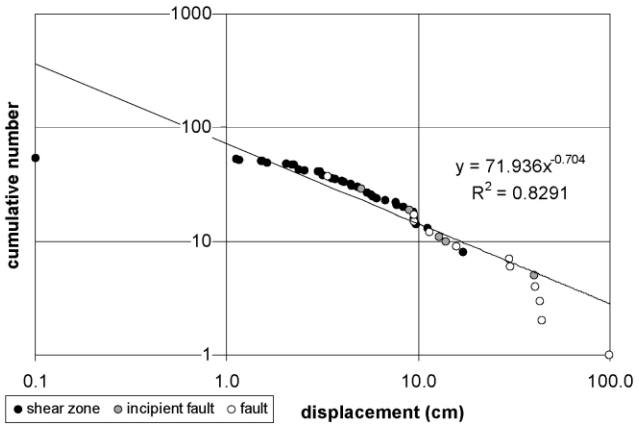

Fig. 6. Population graph of cumulative number vs. displacement for the analysed structures (54 data).

(N) vs. displacement shows a data point distribution, which can be approximated by a straight line segment spanning for more than one order of magnitude (Fig. 6).

4. Discussion and concluding remarks

Based on the analysis presented in the previous section, it appears that displacement and shear strain exert a major control on fault initiation by the coalescence of en-échelon vein arrays in the studied limestones. Critical values of displacement ($D \approx 9$ cm) and shear strain ($\gamma \approx 1.2$) can be determined for the onset of normal fault nucleation from 'brittle–ductile' shear zones in these rocks. The process of fault initiation mostly takes place for displacement values of $9 < D < 17$ cm and shear strain in the range of $1.2 < \gamma < 2.7$.

Shear zones characterised by $D < 9$ cm and $\gamma < 1.2$ consist, with very few exceptions (Fig. 5 and Table 1), of the classic 'brittle–ductile' features described by Ramsay and Graham (1970) and Ramsay and Huber (1987). The deformation processes responsible for the formation of these structures are very likely to be of dominant viscous type (i.e. intracrystalline deformation, pressure solution-crystallisation), obviously accompanied by brittle fracturing (as shown by the coeval formation of tensile cracks). Viscous deformation processes, of both linear (solution mass transfer) and/or power-law type (dislocation glide, dislocation creep) are likely to become progressively less important as discontinuous shear-parallel fractures, characterising the incipient stages of fault nucleation, start to form. Eventually, once through-going faults are well developed, deformation becomes of essentially frictional type. In this context, during incipient fault nucleation ($9 < D < 17$ cm and $1.2 < \gamma < 2.7$), a transition from a dominant viscous to a frictional behaviour occurs.

Displacement data from the analysed shear zone population indicate that this parameter is self-similar for more than one order of magnitude (Fig. 6). Similar power-law relationships are well established for normal fault populations, which tend to be self-similar over a range of scales (e.g. Walsh and Watterson, 1988; Knott et al., 1996; Needham et al., 1996; Yielding et al., 1996 and references therein). Therefore, it seems that, in this respect, 'brittle–ductile' shear zones dominated by viscous deformation processes (accompanied by brittle fracturing) display a behaviour of the type generally shown by faults in the frictional regime.

It is worthy of note that, in Fig. 6, the transition from 'brittle–ductile' shear zones to fully developed faults is not marked by a significant deviation in the straight line trend. Such a deviation occurs instead at the extreme right-hand side of the diagram. This 'tail' of the graph, consisting exclusively of broken (i.e. faulted) shear zones, may be the result of truncation, i.e. undersampling of structures showing relatively large displacements. In fact, only a few structures showing displacements above 40 cm are exposed in the quarry and so an incomplete sampling of this part of the population may have been made. Alternatively, it could be speculated that the deviation of the larger displacement values from the trend seen in the smaller displacement values might correspond to a separate population of larger faults. A possible interpretation could be that, once completely developed, through-going discrete faults can take up relatively large displacements, substantially departing from the trend characterising the early stages of fault initiation from 'brittle–ductile' shear zones. The larger faults could themselves follow a power law, but with a different exponent to the smaller incipient faults and shear zones (e.g. Wojtal, 1994). Clearly, the very few data points in the 'tail' of the diagram in Fig. 6 are statistically not significant to distinguish between these two alternative hypotheses.

Our results, relative to normal fault initiation from shear zones in limestones deformed at very low-grade conditions, should hopefully be relevant to the analysis of fault growth processes within the upper crust. Despite the likely variability of environmental parameters (such as confining pressure, temperature, pore fluid pressure, strain rate) at which en-échelon vein arrays formed in different areas and rock types, these structures tend to maintain similar basic characteristics. The occurrence, within a single outcrop such as that of the present study, of vein arrays showing different degrees of structural evolution and fracture linkage is a commonly observed feature (e.g. Kelly et al., 1998). It suggests that the transition from 'brittle–ductile' to fully brittle shear is unlikely to be merely controlled by an overall increase, occurring at some stage of the structural evolution, of the strain rate at which bulk ('regional') deformation is taking place. On the other hand, for the structures investigated in this study, fluid inclusion analysis (Invernizzi, 2002) appears to rule out the hypothesis that the same transition was triggered by changing burial and temperature conditions, e.g. during ongoing exhumation. As a result, the fundamental role played by finite strain in

the process of fault nucleation from en-échelon vein arrays—at roughly constant environmental conditions—is pointed out. It should be noted that the role of finite strain in triggering brittle fracturing is well established and somewhat intrinsic in rock deformation dominated by mechanisms such as that of low-temperature plasticity (e.g. Frost and Ashby, 1982). The 'brittle–ductile' shear zones analysed in this study developed at temperatures (130–140 °C; Invernizzi, 2002) actually favouring low-temperature deformation in fine grained limestones. More in general, the development of en-échelon vein arrays and their evolution as shear zones (and eventually faults) imply a mixed brittle–ductile behaviour (Ramsay and Huber, 1987) that is compatible with a deformation regime in which low-temperature plasticity plays some role. Such a deformation regime, in turn, may characterise different crustal levels depending on parameters such as strain rate, rock composition and grain size (e.g. Nicolas and Poirier, 1976). As a consequence, finite strain might exert a major control on the process of fault initiation from 'brittle–ductile' shear zones in a wide range of cases, characterised by various environmental (P–T) conditions.

Further analyses may be carried out in rocks characterised by various rheological behaviours and/or deformed under different environmental conditions, to verify the occurrence of critical shear strain values for fault initiation by the coalescence of en-échelon arrays of tensile cracks. Such studies might confirm the role of finite strain in controlling the change in mechanical behaviour implied by the transition from dominantly viscous to frictional deformation. This may be useful to implement existing models of fault nucleation, thereby improving our understanding of the processes that rule the early stages of fault development.

Acknowledgements

The paper greatly benefited from the thorough and constructive reviews by an anonymous referee and M.A. Martins-Neto. We also wish to thank F. Borraccini, G. Cello, C. Invernizzi, L. Marchegiani, L. Mattioni, P. Shiner, E. Tavarnelli and E. Tondi for the stimulating discussions and their useful comments. S.M. was enthusiastically inspired by John Ramsay to work on these topics at his ETH-Zurich times. Projections of orientation data were made using STEREOPLOT (by Neil Mancktelow). Financial support by the University of Urbino and the National Seismic Survey, Rome, are gratefully acknowledged.

References

Bathurst, R.G.C., 1971. Carbonate Sediments and Their Diagenesis, Elsevier, Amsterdam.

Beach, A., 1975. The geometry of en-échelon vein arrays. Tectonophysics 28, 245–263.

Cello, G., Mazzoli, S., 1999. Apennine tectonics in southern Italy: a review. Journal of Geodynamics 27, 191–211.

Cox, S.J.D., Scholz, C.H., 1988a. An experimental study of shear fracture in rocks: mechanical observations. Journal of Geophysical Research 93, 3307–3320.

Cox, S.J.D., Scholz, C.H., 1988b. On the formation and growth of faults. Journal of Structural Geology 10, 413–430.

Etchecopar, A., Granier, T., Larroque, J.-M., 1986. Origin des fentes en echelon: propagation des failles. Compte Rendue de l'Academie de Science de Paris 302, 479–484.

Frost, H.S., Ashby, M.F., 1982. Deformation-mechanism Maps, Pergamon Press, Oxford.

Invernizzi, C., 2002. Utilizzo delle inclusioni fluide nella ricostruzione della storia deformativa: l'esempio di Marsico Nuovo (Appennino meridionale). Studi Geologici Camerti 2002/2 in press.

Kelly, P.G., Sanderson, D.J., Peacock, D.C.P., 1998. Linkage and evolution of conjugate strike-slip fault zones in limestones of Somerset and Northumbria. Journal of Structural Geology 20, 1477–1493.

Knipe, R.J., White, S.H., 1979. Deformation in low grade shear zones in Old Red Sandstone, SW Wales. Journal of Structural Geology 1, 53–66.

Knott, S.D., Beach, A., Brockbank, P.J., Brown, J.L., McCallum, J.E., Welbon, A.I., 1996. Spatial and mechanical controls on normal fault populations. Journal of Structural Geology 18, 359–372.

McGrath, A., Davison, I., 1995. Damage zone geometry around fault tips. Journal of Structural Geology 17 (7), 1011–1024.

Mazzoli, S., Barkham, S., Cello, G., Gambini, R., Mattioni, L., Shiner, P., Tondi, E., 2001. Reconstruction of continental margin architecture deformed by the contraction of the Lagonegro Basin, southern Apennines, Italy. Journal of the Geological Society of London 158, 309–319.

Needham, T., Yielding, G., Fox, R., 1996. Fault population and prediction using examples from the offshore UK. Journal of Structural Geology 18, 155–167.

Nicolas, A, Poirier, J.-P., 1976. Crystalline Plasticity and Solid State Flow in Metamorphic Rocks, Wiley, New York.

Olson, J.E., Pollard, D.D., 1991. The initiation and growth of en échelon veins. Journal of Structural Geology 13, 595–608.

Peacock, D.C.P., Sanderson, D.J., 1995. Pull-aparts, shear fractures and pressure solution. Tectonophysics 241, 1–13.

Pollard, D.D., Segall, P., Delaney, P.T., 1982. Formation and interpretation of dilatant échelon cracks. Geological Society of America Bulletin 93, 1291–1303.

Price, N.J., Cosgrove, J.W., 1990. Analysis of Geological Structures, Cambridge University Press, Cambridge.

Ramsay, J.G., Graham, R.H., 1970. Strain variations in shear belts. Canadian Journal of Earth Sciences 7, 786–813.

Ramsay, J.G., Huber, M.I., 1987. The Techniques of Modern Structural Geology. Volume 2: Folds and Fractures, Academic Press, London.

Roering, C., 1968. The geometrical significance of natural en-échelon crack arrays. Tectonophysics 5, 107–123.

Scholz, C.H., 1990. The Mechanics of Earthquakes and Faulting, Cambridge University Press, Cambridge.

Smith, J.V., 1995. True and apparent geometric variability in en-échelon vein arrays. Journal of Structural Geology 17, 1621–1626.

Smith, J.V., 1996. Geometry and kinematics of convergent conjugate vein array systems. Journal of Structural Geology 18, 1291–1300.

Smith, J.V., 1997. Initiation of convergent extension fracture vein arrays by displacement of discontinuous fault segments. Journal of Structural Geology 19 (11), 1369–1373.

Walsh, J.J., Watterson, J., 1988. Analysis of the relationship between displacements and dimensions of faults. Journal of Structural Geology 10, 239–247.

Willemse, E.J.M., Peacock, D.C.P., Aydin, A., 1997. Nucleation and

growth of strike-slip faults in limestones from Somerset, UK. Journal of Structural Geology 19, 1461–1477.

Wojtal, S.F., 1994. Fault scaling laws and the temporal evolution of fault systems. Journal of Structural Geology 16, 603–612.

Yielding, G., Needham, T., Jones, L., 1996. Sampling of fault population using sub-surface data: a review. Journal of Structural Geology 18, 135–146.